

Submit a Manuscript: <https://www.f6publishing.com>*World J Gastroenterol* 2022 August 28; 28(32): 4649-4667

DOI: 10.3748/wjg.v28.i32.4649

ISSN 1007-9327 (print) ISSN 2219-2840 (online)

ORIGINAL ARTICLE

**Basic Study**

## Anoctamin 5 regulates the cell cycle and affects prognosis in gastric cancer

Tomoyuki Fukami, Atsushi Shiozaki, Toshiyuki Kosuga, Michihiro Kudou, Hiroki Shimizu, Takuma Ohashi, Tomohiro Arita, Hirotaka Konishi, Shuhei Komatsu, Takeshi Kubota, Hitoshi Fujiwara, Kazuma Okamoto, Mitsuo Kishimoto, Yukiko Morinaga, Eiichi Konishi, Eigo Otsuji

**Specialty type:** Gastroenterology and hepatology

Tomoyuki Fukami, Atsushi Shiozaki, Toshiyuki Kosuga, Michihiro Kudou, Hiroki Shimizu, Takuma Ohashi, Tomohiro Arita, Hirotaka Konishi, Shuhei Komatsu, Takeshi Kubota, Hitoshi Fujiwara, Kazuma Okamoto, Eigo Otsuji, Division of Digestive Surgery, Department of Surgery, Kyoto Prefectural University of Medicine, Kyoto 602-8566, Japan

**Provenance and peer review:**

Unsolicited article; Externally peer reviewed.

Mitsuo Kishimoto, Department of Pathology, Kyoto City Hospital, Kyoto 604-8845, Japan

**Peer-review model:** Single blind

Yukiko Morinaga, Eiichi Konishi, Department of Pathology, Kyoto Prefectural University of Medicine, Kyoto 602-8566, Japan

**Peer-review report's scientific quality classification**

Grade A (Excellent): 0

Grade B (Very good): B

Grade C (Good): C, C

Grade D (Fair): 0

Grade E (Poor): 0

**Corresponding author:** Atsushi Shiozaki, MD, PhD, Assistant Professor, Division of Digestive Surgery, Department of Surgery, Kyoto Prefectural University of Medicine, 465 Kajii-cho, Kamigyo-ku, Kyoto 602-8566, Japan. [shiozaki@koto.kpu-m.ac.jp](mailto:shiozaki@koto.kpu-m.ac.jp)

### Abstract

#### BACKGROUND

Anoctamin 5 (ANO5)/transmembrane protein 16E belongs to the ANO/transmembrane protein 16 anion channel family. ANOs comprise a family of plasma membrane proteins that mediate ion transport and phospholipid scrambling and regulate other membrane proteins in numerous cell types. Previous studies have elucidated the roles and mechanisms of ANO5 activation in various cancer types. However, it remains unclear whether ANO5 acts as a plasma membrane chloride channel, and its expression and functions in gastric cancer (GC) have not been investigated.

#### AIM

To examine the role of ANO5 in the regulation of tumor progression and clinicopathological significance of its expression in GC.

#### METHODS

Knockdown experiments using ANO5 small interfering RNA were conducted in human GC cell lines, and changes in cell proliferation, cell cycle progression, apoptosis, and cellular movement were assessed. The gene expression profiles of GC cells were investigated following ANO5 silencing by microarray analysis. Immunohistochemical staining of ANO5 was performed on 195 primary tumor



samples obtained from patients with GC who underwent curative gastrectomy between 2011 and 2013 at our department.

## RESULTS

Reverse transcription-quantitative polymerase chain reaction (PCR) and western blotting demonstrated high ANO5 mRNA and protein expression, respectively, in NUGC4 and MKN45 cells. In these cells, ANO5 silencing inhibited cell proliferation and induced apoptosis. In addition, the knockdown of ANO5 inhibited G<sub>1</sub>-S phase progression, invasion, and migration. The results of the microarray analysis revealed changes in the expression levels of several cyclin-associated genes, such as CDKN1A, CDK2/4/6, CCNE2, and E2F1, in ANO5-depleted NUGC4 cells. The expression of these genes was verified using reverse transcription-quantitative PCR. Immunohistochemical staining revealed that high ANO5 expression levels were associated with a poor prognosis. Multivariate analysis identified high ANO5 expression as an independent prognostic factor for 5-year survival in patients with GC ( $P = 0.0457$ ).

## CONCLUSION

ANO5 regulates the cell cycle progression by regulating the expression of cyclin-associated genes and affects the prognosis of patients with GC. These results may provide insights into the role of ANO5 as a key mediator in tumor progression and/or promising prognostic biomarker for GC.

**Key Words:** Anoctamin 5; Gastric cancer; Cell cycle; G1/S checkpoint; Cell proliferation

©The Author(s) 2022. Published by Baishideng Publishing Group Inc. All rights reserved.

**Core Tip:** The present study aimed to investigate the role of anoctamin 5 (ANO5) in the regulation of tumor progression and the clinicopathological significance of its expression in gastric cancer. Immunohistochemical staining revealed that high ANO5 expression levels were associated with a poor prognosis in patients with gastric cancer. Microarray analysis results suggest that ANO5 regulates cell cycle progression by regulating the expression of cyclin-associated genes. Our results provide insights into the role of ANO5 as a mediator of and/or biomarker for gastric cancer.

**Citation:** Fukami T, Shiozaki A, Kosuga T, Kudou M, Shimizu H, Ohashi T, Arita T, Konishi H, Komatsu S, Kubota T, Fujiwara H, Okamoto K, Kishimoto M, Morinaga Y, Konishi E, Otsuji E. Anoctamin 5 regulates the cell cycle and affects prognosis in gastric cancer. *World J Gastroenterol* 2022; 28(32): 4649-4667

**URL:** <https://www.wjgnet.com/1007-9327/full/v28/i32/4649.htm>

**DOI:** <https://dx.doi.org/10.3748/wjg.v28.i32.4649>

## INTRODUCTION

The anoctamin (ANO)/transmembrane protein 16 (TMEM16) family is present in numerous eukaryotes, and ten ANO paralogs, ANO1-ANO10 (TMEM16A-H, TMEM16J and K), have been identified in vertebrates[1]. Of these, several function as calcium-activated chloride channels. ANOs comprise a family of plasma membrane proteins that mediate ion transport, phospholipid scrambling, and other membrane protein regulation in numerous cell types[2-6]. Their expression has been detected in both epithelial and non-epithelial tissues types[4]. Although the regulation of ANOs has been extensively examined, the mechanisms by which increased intracellular calcium concentration activates chloride or cation conductance have not been elucidated.

Recent molecular and biochemical studies reported a role for ANOs in human carcinogenesis. For instance, the expression of ANO proteins is upregulated in cancer and associated with a poor patient prognosis[7]. A relationship has been demonstrated between ANO1 and patient prognosis in various cancer types, including gastric, esophageal, breast, lung, and head and neck cancer[8-12]. The upregulation of the genes encoding ANO1 and ANO3 has been associated with several cancer types, specifically gastrointestinal stromal tumors, breast cancer, and squamous cell carcinoma[12,13]. Furthermore, ANO6 has been strongly implicated in the metastatic potential of breast cancer[14]. The expression levels of other members of the ANO family are also associated with cell proliferation and cancer development[15-17].

In our previous studies, we identified a crucial role for several chloride ion channels and transporters in patients with gastric cancer (GC); intracellular chloride regulates proliferation and cell cycle progression[18,19], whereas furosemide, a potent inhibitor of the Na<sup>+</sup>/K<sup>+</sup>/2Cl<sup>-</sup>cotransporter, induces G<sub>0</sub>/G<sub>1</sub> arrest[20]. Furthermore, leucine rich repeat containing 8 VRAC subunit A regulate the proliferation,

apoptosis, migration, and invasion of GC cells[21].

ANO5 has recently been implicated in various cancers, such as thyroid[22] and pancreatic cancer[23]; however, limited information is presently available on its involvement in tumor progression in patients with GC or the clinical significance of its expression. Therefore, in the present study, we investigated whether ANO5 contributes to the regulation of cancer growth and evaluated its clinicopathological significance in GC.

## MATERIALS AND METHODS

### **Cell lines, antibodies**

MKN7, MKN45, MKN74, HGC27, and NUGC4 human GC cell lines were purchased from the Riken Cell Bank (Tsukuba, Japan). Cells were cultured in RPMI-1640 (Nacalai Tesque, Kyoto, Japan) containing 100 µg/mL of streptomycin, 100 U/mL penicillin, and 10% FBS at 37 °C in a 5% CO<sub>2</sub> incubator. Rabbit polyclonal anti-ANO5 antibody was obtained from Funakoshi (GTX81161) for immunohistochemical (IHC) analysis and western blotting. Mouse monoclonal anti-β-actin antibody was provided by Sigma-Aldrich (St. Louis, MO, United States) and HRP-conjugated anti-rabbit and mouse secondary antibodies by Cell Signaling Technology (Beverly, MA, United States).

### **Reverse transcription-quantitative polymerase chain reaction**

RNA was extracted from cancer cells using an RNeasy kit (Qiagen, Valencia, CA, United States). The Step One plus™ Real-Time polymerase chain reaction (PCR) System (Applied Biosystems, Foster City, CA, United States) and TaqMan Gene Expression Assays (Applied Biosystems) were employed for reverse transcription-quantitative PCR analysis using the following PCR thermocycling conditions: initial denaturation step at 95 °C for 10 min, followed by 40 cycles at 95 °C for 15 s and 60 °C for 1 min. The expression levels of the following genes were assessed: ANO5 (Hs01381106\_m1), CDKN1A (Hs00355782\_m1), CDK2 (Hs00608082\_m1), CDK4 (Hs00175935\_m1), CDK6 (Hs00608037\_m1), cyclin E2 (CCNE2; Hs00180319\_m1), and E2F1 (Hs00153451\_m1) (all from Applied Biosystems). The expression of each gene was normalized using the housekeeping gene β-actin (Hs01060665\_g1; Applied Biosystems). All assays were performed in triplicates.

### **Western blotting**

The cells were washed twice with ice-cold PBS and harvested in M-PER lysis buffer (Pierce, Rockford, IL, United States) supplemented with protease inhibitors (Pierce Biotechnology). Protein concentrations were measured using a modified Bradford assay (Bio-Rad, Hercules, CA, United States). Cell lysates containing equal amounts of total protein (10 mg/lane) were resolved using 10% SDS-PAGE and subsequently transferred to polyvinylidene fluoride membranes (GE Healthcare, Piscataway, NJ, United States). Membranes were incubated with antibodies for 24 h at 4 °C. Band densities were quantified using ImageJ (version 1.52; National Institutes of Health).

### **Small interfering RNA transfection**

All small interfering RNA (siRNA) reverse transfection procedures were performed using Lipofectamine® RNAiMAX reagent (Invitrogen, Carlsbad, CA, United States) with a final siRNA concentration of 20 nmol/L, according to the manufacturer's instructions. ANO5 siRNA (Stealth RNAi siRNA; HSS137119, Stealth RNAi siRNA; HSS137120) and control siRNA (Stealth RNAiTM siRNA Negative Control) were obtained from Invitrogen.

### **Overexpression study**

Control-HaloTag® plasmid (Promega, G6591) and ANO5-HaloTag® plasmid (pFN21AE5809) were transfected using P3000TM (Invitrogen) and lipofectamine 3000 (Invitrogen) following the manufacturer's instructions. After passaging, ANO5-expressing cells were used for the cell proliferation assay.

### **Cell proliferation assay**

NUGC4 and MKN45 cells were seeded at densities of 1.0 and 2.0 × 10<sup>5</sup> cells/well, respectively, on six-well plates and incubated at 37 °C in a 5% CO<sub>2</sub> incubator. The siRNA was transfected 24 h after seeding. The cells were detached from the plates with trypsin-EDTA 48 h and 72 h after siRNA transfection and counted using a hemocytometer.

Cell proliferation activity was measured using the water-soluble tetrazolium salts-8 assay with Cell Count Reagent SF (Nacalai Tesque). NUGC4, MKN45, and MKN7 cells were seeded at a density of 1.0 × 10<sup>4</sup>, 1.0 × 10<sup>4</sup>, and 1.5 × 10<sup>4</sup> cells/well, respectively, in 24-well plates and were incubated at 37 °C in a 5% CO<sub>2</sub> incubator. The siRNA was transfected 24 h after seeding. Cell proliferation was evaluated every 24 h by measuring the absorbance at 450 nm using a Thermo Scientific Multiskan FC (Thermo Fisher Scientific).

### Cell cycle assay

Cell cycle progression was assessed 48 h after siRNA transfection by flow cytometry. Cells were detached from the plates using trypsin-EDTA and subsequently treated with 0.2% Triton X-100 and stained with propidium iodide with RNase staining buffer (BD Biosciences, San Jose, CA, United States). Flow cytometry data were acquired using a BD Accuri C6 plus flow cytometer (BD Biosciences) to assess DNA content in at least 10000 cells.

### Apoptosis assay

Cells were evaluated 72 h after transfection and stained using the ANNEXIN V-FITC Kit (Beckman Coulter, Brea, CA, United States). The frequencies of early and late apoptotic cells among at least 10000 cells were assessed using a BD Accuri C6 plus flow cytometer.

### Migration and invasion assays

Migration assays were performed using 24-well cell culture inserts with 8- $\mu$ m pores (BD Biosciences), whereas invasion assays were performed using Biocoat Matrigel® (BD Biosciences). At 48 h post-transfection, NUGC4 and MKN45 cells were seeded at a density of  $3.0 \times 10^5$  cells/well in serum-free RPMI-1640 in the upper chamber, whereas the lower chamber contained RPMI-1640 with 10% FBS. Matrigel and the cells remaining in the upper chamber after a 48-h incubation were removed. Diff-Quick staining reagents (Sysmex) were used to stain migrated or invaded cells, which were counted in four independent fields of view. Both assays were conducted thrice.

### Microarray analysis

NUGC4 and MKN45 cells were transfected with either control or ANO5 siRNA. At 48 h after siRNA transfection, total RNA was extracted using RNeasy kit. Cyanine 3 (Cy3)-labeled cRNA was prepared from 0.1  $\mu$ g total RNA using the Low Input Quick Amp Labeling Kit (Agilent Technologies, CA, United States) and then subjected to RNeasy column purification (Qiagen). Dye incorporation and cRNA yields were assessed using a NanoDrop 2000 Spectrophotometer (Thermo Fisher Scientific). Subsequently, 0.6  $\mu$ g Cy3-labeled cRNA was fragmented in a 25  $\mu$ L reaction volume containing 1  $\times$  Agilent fragmentation buffer and 2  $\times$  Agilent blocking agent at 60 °C for 30 min. The 2  $\times$  Agilent hybridization buffer (25  $\mu$ L) was then added, and hybridization to SurePrint G3 Human GE 8  $\times$  60K Microarray Ver3.0 (Agilent Technologies) was conducted at 65 °C for 17 h in a rotating Agilent hybridization oven. The microarrays were then washed with GE Wash Buffer 1 (Agilent Technologies) at room temperature for 1 min, followed by GE Wash buffer 2 (Agilent Technologies) at 37 °C for 1 min.

### Microarray data processing

Slides were scanned using the Agilent SureScan Microarray Scanner (G2600D) with the one color scan setting for 8  $\times$  60k array slides. The scanned images were analyzed with Feature Extraction Software (Agilent Technologies) using the default parameters to obtain background-subtracted and spatially detrended processed signal intensities. Microarray data were analyzed using ingenuity pathway analysis software (Ingenuity Systems, Redwood City, CA).

### Patients and primary tissue samples

Histologically proven primary GC tumor samples were obtained from 195 consecutive patients who underwent curative gastrectomy between 2011 and 2013 at Kyoto Prefectural University of Medicine, Japan. For mRNA analysis, frozen tissue samples of normal stomach and tumors were collected from surgical specimens and stored at -80 °C. Written informed consent was obtained from all patients prior to enrollment. Patients with noncurative resection or preoperative chemotherapy were excluded from the study. Tumor staging was conducted according to the International Union Against Cancer/TNM Classification of Malignant Tumors (8<sup>th</sup> edition)[24]. The present study was approved by the Institutional Review Board of the Kyoto Prefectural University of Medicine (ERB-C-1195).

### IHC

The Vectastain avidin-biotinylated peroxidase complex Elite Kit (Vector Laboratories, Burlingame, CA, United States) was employed for IHC staining using the avidin-biotinylated peroxidase complex method. After deparaffinization in xylene, sections were rehydrated in a graded series of ethanol solutions. The sections were then incubated in 0.3% H<sub>2</sub>O<sub>2</sub> for 30 min to block endogenous peroxidase activity. Endogenous biotin, biotin receptors, and avidin-binding sites were also blocked using an Avidin/Biotin Blocking Kit (Vector laboratories). Sections were incubated with ANO5 antibody diluted 1:100 at 37 °C for 1 h and then at 4 °C overnight. Cells were visualized using the standard avidin-biotinylated peroxidase complex method, with hematoxylin as the counterstain.

ANO5 expression levels in immunohistochemically stained samples were semi-quantitatively graded based on the staining intensity and proportion of cytoplasm in the stained cancer cells. The staining intensity was scored as 0 (no staining), 1 (weak staining), 2 (moderate staining), or 3 (strong staining). The proportion of stained tumor cells as a percentage of the stained area in the cancer area was scored

from 0 to 1.0. IHC scores were calculated as the maximum multiplied product of intensity and proportion scores (0-3.0). IHC diagnosis was based on tumor ANO5 expression assessment, and other IHC parameters were performed by at least two physicians, including an experienced pathologist.

#### **Quantification of intracellular chloride concentration and low chloride stimulation**

MQAE reagent, a chloride-sensitive fluorescence probe (Dojindo Laboratories, Kumamoto, Japan) was used to assess intracellular chloride concentrations. NUGC4 and MKN45 cells were seeded in 24-well plates at a density of  $3.0 \times 10^4$  cells/well and then incubated in normal medium at 37 °C with 5% CO<sub>2</sub>. The medium was then replaced with standard and low-chloride medium in which MQAE was dissolved, and cells were incubated at 37 °C in a CO<sub>2</sub> incubator for a further 12 h. Following washing with PBS five times, the fluorescence intensity of MQAE was evaluated under a fluorescence microscope (BZ-X800; Keyence, Osaka, Japan). Three fields of view were analyzed *per* sample at  $\times 100$  magnification. Quantification was performed using a BZ-X800 analyzer and accompanying software (BZ-H4C, v.1.1.1.8; Keyence).

A low chloride stimulation experiment was conducted to examine the effects of changes in intracellular chloride concentrations on GC cells. A low-chloride medium supplemented with 10% FBS was prepared in chloride-free RPMI-1640 (chloride replaced with NO<sub>3</sub><sup>-</sup>) (Nacalai Tesque).

#### **c-Jun N-terminal kinase signaling pathway inhibitor treatment**

To block the c-Jun N-terminal kinase (JNK) signaling pathway, NUGC4 and MKN45 cells were incubated with the JNK inhibitor SP600125 (10 μm, ab120065, Abcam) according to manufacturer's instructions. The cells were divided into 3 groups: control, ANO5 siRNA, and JNK inhibitor (ANO5 siRNA + SP600125). Cell proliferation was detected every 24 h after ANO5 silencing.

#### **Statistical analysis**

Statistical analysis was performed using the Mann-Whitney *U* test for two-group comparisons. Categorical data were analyzed using Fisher's exact test. The Kaplan-Meier method was used to construct survival curves, and differences in survival were examined using the log-rank test for equality. Prognostic factors were identified using the Cox proportional hazard model. These analyses were performed using the JMP statistical software (version 15; SAS Institute, Cary, NC, United States). Data are presented in the graphs as the mean ± standard error of the mean. *P* < 0.05 was considered a statistically significant difference.

---

## **RESULTS**

#### **ANO5 expression in GC cells**

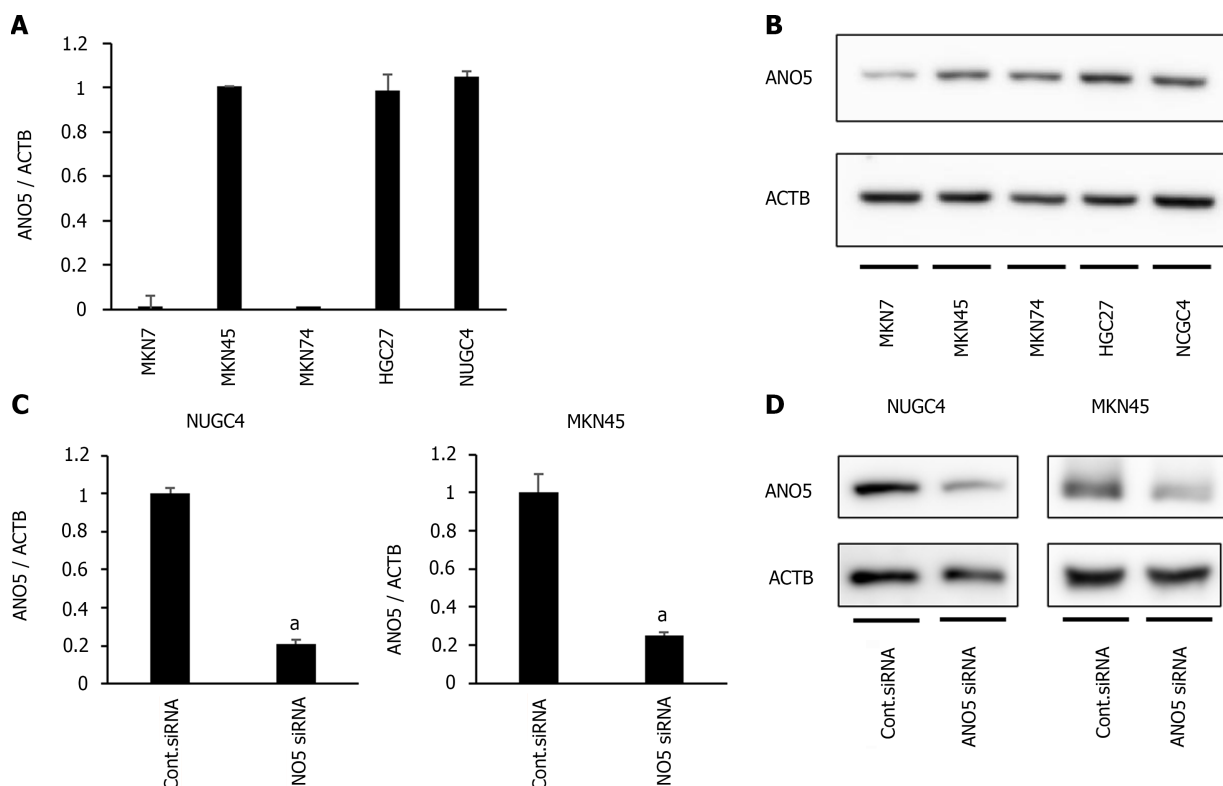
ANO5 gene and protein expression were first examined in five human GC cell lines, MKN7, MKN45, MKN74, HGC27, and NUGC4, by reverse transcription-quantitative PCR and western blotting. ANO5 expression was detected in several cells in the five GC cell lines (Figure 1A and B). Compared to paired adjacent normal tissue, ANO5 expression was significantly upregulated in GC tissue (*P* = 0.004; *n* = 12; Supplementary Figure 1).

ANO5 expression was knocked down using siRNA in NUGC4 and MKN45 cells, and its effects on tumor progression were assessed. ANO5 mRNA (Figure 1C) and protein levels (Figure 1D) were downregulated in NUGC4 and MKN45 cells. We also conducted an overexpression study in MKN7 cells. The ANO5 plasmid increased ANO5 mRNA levels (Supplementary Figure 2A, left panel).

#### **ANO5 regulates cell growth and survival in GC cells**

The effect of ANO5 siRNA transfection on the proliferation and cell cycle progression of NUGC4 and MKN45 cells were subsequently examined. Compared with the control siRNA, the number of NUGC4 and MKN45 cells was significantly reduced at 48 h and 72 h after the transfection with ANO5 siRNA (Figure 2A, left panel). The results of the cell proliferation assay showed that the relative absorbance of GC cells transfected with the control siRNA (NUGC4 and MKN45) was significantly lower than that of GC cells transfected with ANO5 siRNA (HSS137119) (NUGC4 and MKN45) (Figure 2A, right panel). Whereas, ANO5 plasmid increased the relative absorbance of MKN7 cell (Supplementary Figure 2B). Moreover, ANO5 silencing increased the numbers of NUGC4 and MKN45 cells in the G<sub>0</sub>/G<sub>1</sub> phase (Figure 2B). These results indicated that ANO5 regulated the proliferation and cell cycle of GC cells.

To further clarify the role of ANO5, apoptosis assays were performed in NUGC4 and MKN45 cells. ANO5 silencing significantly increased the frequency of early and late apoptotic NUGC4 cells and the frequency of early apoptotic MKN45 cells 72 h after siRNA transfection (Figure 3A). These results indicated that the apoptosis in NUGC4 and MKN45 cells was regulated by ANO5 expression. Another ANO5 siRNA (HSS137120) was used to assess its impact on cell growth and survival, with results similar to those of HSS137119 (Supplementary Figure 3).



DOI: 10.3748/wjg.v28.i32.4649 Copyright ©The Author(s) 2022.

**Figure 1** Anoctamin 5 expression in gastric cancer cells. **A:** Real-time quantitative reverse transcription-quantitative polymerase chain reaction (PCR) showed the expression of anoctamin 5 (ANO5) in various cell lines in gastric cancer; **B:** Western blotting showed the expression of ANO5 in various cell lines in GC; **C:** Real-time quantitative PCR revealed that ANO5 small interfering RNA (siRNA) effectively reduced ANO5 mRNA levels in NUGC4 and MKN45 cells; **D:** Western blotting revealed that ANO5 siRNA effectively reduced ANO5 protein levels in NUGC4 and MKN45 cells.  $n = 3$ , mean  $\pm$  standard error of the mean.  $^aP < 0.05$  (significantly different from control siRNA). ANO5: Anoctamin 5; ACTB:  $\beta$ -actin; siRNA: Small interfering RNA.

### ANO5 promotes the migration and invasion

The effects of the ANO5 silencing on NUGC4 and MKN45 cell migration and invasion were examined using a Boyden chamber assay. The results demonstrated that ANO5 knockdown in NUGC4 and MKN45 cells significantly reduced their migration and invasion (Figure 3B).

### Gene expression profiling in ANO5 siRNA-transfected NUGC4 cells

To elucidate the molecular mechanisms underlying the regulation of cellular functions by ANO5, the gene expression profiles of NUGC4 cells transfected with ANO5 siRNA were investigated using microarray. The results revealed that the expression levels of 3491 genes in NUGC4 cells following ANO5 knockdown exhibited fold-changes  $> 1.8$  compared with those in the negative control. Among these, the expression levels of 1802 genes were upregulated, whereas those of 1689 genes were downregulated in NUGC4 cells following ANO5 knockdown. The top 20 genes with significant changes in expression in the ANO5-depleted NUGC4 cells are listed in Tables 1 and 2. Ingenuity pathway analysis showed that 'Cancer' was the top-ranked disease and disorder, while 'DNA Replication, Recombination, and Repair' and 'Cell Cycle' were the two top-ranking molecular and cellular functions (Table 3).

### Validation of gene and protein expression

The microarray analysis identified 'Cell Cycle: G1/S Checkpoint Regulation' as one of the top-ranking canonical pathways in ANO5-depleted NUGC4 cells (Figure 4A). To confirm these results, seven genes were selected (CDK2, CDK4, CDK6, CDKN1A/p21, CCNE2, E2F1, and Rb). These genes were included in 'Cell Cycle: G1/S Checkpoint Regulation,' and CDK2 and CDK6 were the two top-ranking downregulated genes in NUGC4 cells following ANO5 knockdown (Table 2). Reverse transcription-quantitative PCR was used to confirm the expression levels of six genes. NUGC4 and MKN45 cells transfected with ANO5 siRNA had significantly lower CDK2, CDK4, CDK6, CDKN1A, CCNE2, and E2F1 expression levels and significantly higher CDKN1A expression levels than cells transfected with the control siRNA (Figure 4B). Furthermore, ANO5 plasmid decreased CDKN1A/p21 mRNA levels (Supplementary Figure 2A, right panel). Western blotting revealed that phosphorylated Rb was inhibited following ANO5 knockdown in NUGC4 and MKN45 cells (Figure 4C). Since the CDK2 gene is located upstream of Rb and downstream of p21 in the cell cycle transition from G<sub>1</sub> phase to S phase, the downregulation of

**Table 1 The 20 upregulated genes that displayed the greatest changes in their expression in anoctamin 5-depleted NUGC4 cells**

Gene symbol	Gene name	Gene ID	Fold change
PLCXD1	<i>Phosphatidylinositol-specific phospholipase C X domain containing 1</i>	TC0X00006433.hg.1	31.97
NDRG4	<i>NDRG family member 4</i>	TC1600008034.hg.1	29.88
CYP3A5	<i>Cytochrome P450 family 3 subfamily A member 5</i>	TC0700011953.hg.1	24.81
PLCXD1	<i>Phosphatidylinositol-specific phospholipase C X domain containing 1</i>	TC0Y00006433.hg.1	23.44
REG4	<i>Regenerating family member 4</i>	TC0100015477.hg.1	19.70
CIDEB	<i>Cell death-inducing DFFA-like effector b</i>	TC1400008752.hg.1	17.86
DHRS9	<i>Dehydrogenase/reductase 9</i>	TC0200009905.hg.1	17.02
CIDEC	<i>Cell death-inducing DFFA-like effector c</i>	TC0300010217.hg.1	16.73
SPRR1A	<i>Small proline rich protein 1A</i>	TC0100010017.hg.1	16.66
APOD	<i>Apolipoprotein D</i>	TC0300013645.hg.1	16.57
SEMA7A	<i>Semaphorin 7A</i>	TC1500010018.hg.1	16.09
C11orf86	<i>Chromosome 11 open reading frame 86</i>	TC1100008109.hg.1	15.57
BNIPL	<i>BCL2 interacting protein like</i>	TC0100009936.hg.1	15.52
SUSD2	<i>Sushi domain containing 2</i>	TC2200006883.hg.1	15.25
MAPRE3	<i>Microtubule-associated protein RP/EB family member 3</i>	TC0200007048.hg.1	14.99
CYP1A1	<i>Cytochrome P450 family 1 subfamily A member 1</i>	TC1500010042.hg.1	14.69
GOLT1A	<i>Golgi transport 1A</i>	TC0100017022.hg.1	13.79
CNN2	<i>Calponin 2</i>	TC1900006507.hg.1	13.74
ANTXR2	<i>ANTXR cell adhesion molecule 2</i>	TC0400011144.hg.1	13.54
APOBEC1	<i>Apolipoprotein B mRNA editing enzyme catalytic subunit 1</i>	TC1200009789.hg.1	12.19

**Table 2 The 20 downregulated genes that displayed the greatest changes in their expression in anoctamin 5-depleted NUGC4 cells**

Gene symbol	Gene name	Gene ID	Fold change
CDK2	<i>Cyclin-dependent kinase 2</i>	TC1200007819.hg.1	-53.84
DTL	<i>Denticleless E3 ubiquitin ligase homolog</i>	TC0100011512.hg.1	-27.60
RABL3	<i>RAB, member of RAS oncogene family like 3</i>	TC0300012157.hg.1	-20.16
CKS1B	<i>CDC28 protein kinase regulatory subunit 1B</i>	TC0100010100.hg.1	-19.34
LMNB1	<i>Lamin B1</i>	TC0500008544.hg.1	-19.18
IFRD2	<i>Interferon-related developmental regulator 2</i>	TC0300013981.hg.1	-18.61
PLK1	<i>Polo like kinase 1</i>	TC1600007235.hg.1	-17.89
GINS1	<i>GINS complex subunit 1</i>	TC2000007016.hg.1	-17.87
CDK6	<i>Cyclin-dependent kinase 6</i>	TC0700011785.hg.1	-17.08
XRCC2	<i>X-ray repair cross complementing 2</i>	TC0700013119.hg.1	-14.77
POGLUT3	<i>Protein O-glucosyltransferase 3</i>	TC1100012229.hg.1	-14.47
DSG2	<i>Desmoglein 2</i>	TC1800007014.hg.1	-14.37
NEMP1	<i>Nuclear envelope integral membrane protein 1</i>	TC1200010946.hg.1	-14.31
CBX5	<i>Chromobox 5</i>	TC1200010833.hg.1	-14.20
ANKRD52	<i>Ankyrin repeat domain 52</i>	TC1200010902.hg.1	-14.20
ITGB1	<i>Integrin subunit beta 1</i>	TC1000010265.hg.1	-14.16
H2BC14	<i>H2B clustered histone 14</i>	TC0600007377.hg.1	-13.25

SCAMP2	<i>Secretory carrier membrane protein 2</i>	TC1500010047.hg.1	-13.05
CMTM7	<i>CKLF like MARVEL transmembrane domain containing 7</i>	TC0300006968.hg.1	-13.02
GINS4	<i>GINS complex subunit 4</i>	TC0800007416.hg.1	-12.66

ANO5 in GC cells appears to affect the transition from the G1 phase to the S phase by regulating the expression of p21 and its downstream genes in signal pathways.

In addition, the gene expression profile of MKN45 cells transfected with ANO5 siRNA was investigated by microarray. Changes in gene expression in ANO5-depleted NUGC4 and MKN45 cells are depicted in **Supplementary Figure 4**. Among the 21440 genes, 7246 genes were upregulated and 6622 genes were downregulated in both cell lines, for a total of 13868 genes (64.7%) with identical expression direction in NUGC4 and MKN45 cells. The direction of gene expression changes of gene related to 'Cell Cycle: G<sub>1</sub>/S Checkpoint Regulation' was consistent in both cell lines (**Supplementary Table 1**). Furthermore, all 40 genes displayed in Tables 1 and 2 showed the identical expression patterns in ANO5-depleted MKN45 cells (**Supplementary Table 2**). These results supported that ANO5 affected the cell cycle through similar mechanisms in both NUGC4 and MKN45 cell lines.

### **ANO5 inhibits the JNK pathway**

Activation of the JNK and p38 MAPK classes of protein kinases mediates cellular responses such as apoptosis and the maturation of some cell types. JNK stabilizes p21 protein through phosphorylation [25]. To elucidate the regulatory role of ANO5 in the JNK signaling pathway in GC cells, we examined the phosphorylation of the JNK protein. ANO5 silencing significantly increased JNK phosphorylation levels in NUGC4 and MKN45 cells (**Figure 4D**). Furthermore, the increase of *CDKN1A/p21* mRNA expression induced by ANO5 silencing in NUGC4 and MKN45 cells was suppressed by JNK inhibition (**Supplementary Figure 5**, lower panel). Whereas, treatment with JNK inhibitors did not affect ANO5 mRNA expression (**Supplementary Figure 5**, upper panel). These results indicated that ANO5 expression regulated the cell cycle by upregulating p21 *via* JNK cascade activation in GC cells.

### **Effects of low-chloride conditions**

To elucidate the molecular mechanisms through which ANO5 affects the cell cycle transition from G<sub>1</sub> to S phase, changes in the intracellular ion environment were examined. A previous study has reported that intracellular chloride affects cancer growth through the phosphorylation of several key molecules in signal transduction pathways[20]. We previously reported that the culturing in a Cl<sup>-</sup>-replaced medium (replacement of Cl<sup>-</sup> by NO<sub>3</sub><sup>-</sup>) decreased the intracellular chloride concentration ([Cl<sup>-</sup>]<sub>i</sub>) and inhibited cell growth in GC cells[19]. Our previous study also demonstrated that JNK activation under low-chloride conditions inhibited GC cell growth by upregulating p21 expression[18]. Intracellular chloride concentrations in the cells were measured based on the fluorescence intensity of MQAE, a chloride-sensitive fluorescence probe. The results revealed an increases in the fluorescence intensity of MQAE in NUGC4 and MKN45 cells following ANO5 knockdown (**Figure 5**). Therefore, ANO5 knockdown altered intracellular chloride concentrations in GC cells. Furthermore, low-chloride conditions effectively increased JNK phosphorylation and reduced Rb phosphorylation (**Supplementary Figure 6**). These results indicated that ANO5 regulated the cell cycle *via* JNK signaling by controlling intracellular chloride levels.

### **IHC analysis of ANO5 expression in human GC tissue**

IHC detected the expression of ANO5 in non-cancerous gastric (**Figure 6A**) and cancerous epithelia (**Figure 6B**). ANO5 was observed to be expressed in the cell membranes and cytoplasm of GC tissue. The criteria for the staining intensity score were defined as 0 (no staining; **Figure 6C**), 1 (weak staining; **Figure 6D**), 2 (moderate staining; **Figure 6E**), or 3 (strong staining; **Figure 6F**). The median and mean scores for ANO5 expression were 0.9 (range, 0-2.1) and 0.97 (standard deviation = 0.53), respectively. A cut-off value of 1.3 was used to obtain the smallest P value in comparison of 5-year overall survival (OS) rates[26]. The 5-year OS rates for each cut-off value are presented in **Table 4**.

Patients with GC were divided into low- (ANO5 scores < 1.3, n = 137) and high-ANO5 (ANO5 scores ≥ 1.3, n = 58) expression groups based on a cut-off value of 1.3 (**Figure 6G**). Analysis of the clinicopathological features revealed that ANO5 expression levels were not associated with any of the variables (**Table 5**). To evaluate the prognostic significance of ANO5 after surgery, the following ten variables were compared: sex, age, tumor location, tumor length, histological type, lymphatic invasion, venous invasion, the pathological T stage, pathological N stage, and ANO5 IHC scores. Univariate analysis showed that patient prognosis was correlated with tumor length, lymphatic invasion, venous invasion, pathological T stage, pathological N stage, and ANO5 IHC scores (P = 0.0020, 0.0002, 0.0126, < 0.0001, < 0.0001, and 0.0104, respectively). Multivariate analysis identified high ANO5 expression (≥ 1.3) as an independent prognostic factor (P = 0.0457) (**Table 6**). Furthermore, the 5-year OS rate was significantly lower in the high expression group (73.9%) than in the low expression group (89.6%). Data obtained from the Kaplan-Meier plotter database also indicated that high ANO5 expression correlates with poor

**Table 3** Ingenuity pathway analysis of anoctamin 5-depleted NUGC4 cells

Category	Name	Molecules	P value (range)
Disease and Disorders	Cancer	3136	$1.54 \times 10^{-3}$ - $2.23 \times 10^{-15}$
	Neurological Disease	76	$1.27 \times 10^{-3}$ - $2.23 \times 10^{-15}$
	Organismal Injury and Abnormalities	3147	$1.54 \times 10^{-3}$ - $2.23 \times 10^{-15}$
	Cardiovascular Disease	138	$1.43 \times 10^{-3}$ - $4.07 \times 10^{-14}$
	Reproductive System Disease	1942	$1.54 \times 10^{-3}$ - $1.09 \times 10^{-10}$
Molecular and Cellular Functions	DNA Replication, Recombination, and Repair	460	$1.54 \times 10^{-3}$ - $9.69 \times 10^{-22}$
	Cell Cycle	650	$1.54 \times 10^{-3}$ - $1.98 \times 10^{-20}$
	Cellular Assembly and Organization	533	$1.57 \times 10^{-3}$ - $9.22 \times 10^{-16}$
	Cellular Development	691	$1.59 \times 10^{-3}$ - $2.66 \times 10^{-14}$
	Cellular Growth and Proliferation	677	$1.40 \times 10^{-3}$ - $2.66 \times 10^{-14}$
Physiological System Development and Function	Connective Tissue Development and Function	60	$1.14 \times 10^{-3}$ - $8.83 \times 10^{-6}$
	Tissue Development	164	$1.57 \times 10^{-3}$ - $1.11 \times 10^{-4}$
	Embryonic Development	80	$1.21 \times 10^{-3}$ - $2.07 \times 10^{-4}$
	Hair and Skin Development and Function	55	$6.37 \times 10^{-4}$ - $2.07 \times 10^{-4}$
	Organ Development	69	$6.37 \times 10^{-4}$ - $2.07 \times 10^{-4}$

**Table 4** Five-year overall survival rates with cut-off values for anoctamin 5 expression scores

Cut-off value	5-yr OS rate		P value
	Low group	High group	
1.0	87.0% (n = 101)	83.7% (n = 94)	0.5136
1.1	87.7% (n = 115)	81.9% (n = 80)	0.2890
1.2	88.8% (n = 127)	78.6% (n = 68)	0.0759
1.3	89.6% (n = 137)	73.9% (n = 58)	0.0104 <sup>a</sup>
1.4	88.1% (n = 142)	78.6% (n = 53)	0.0380 <sup>a</sup>
1.5	87.4% (n = 152)	78.5% (n = 43)	0.0751

<sup>a</sup>P < 0.05: Log-rank test.

OS: Overall survival.

prognosis in GC (Supplementary Figure 7), which was consistent with the present results.

## DISCUSSION

The ANO family of membrane proteins, also known as TMEM16, play key roles in several physiological functions, including ion transport to phospholipid scrambling[27] and ion channel regulation[28]. While the roles of ANO1 (TMEM16A) and ANO2 (TMEM16B) as calcium-activated chloride channels have been firmly established[29-32], the functions of other family members remain unclear.

Previous studies have evaluated the expression and role of ANO5 during tumor development in various cancer types. Song *et al*[33] demonstrated that ANO5 (TMEM16E) was widely expressed in the epithelial cells of the human gastrointestinal tract. ANO5 is also expressed in human pancreatic cancer tissues but not in normal pancreatic tissue[23]. Chang *et al*[22] reported that ANO5 expression was downregulated in thyroid cancer, which promoted thyroid cancer cell migration and invasion. However, the expression of ANO5 in human GC tissue and the pathophysiological role of its expression in GC cells have not been demonstrated.

The present study revealed that ANO5 downregulation in GC cells regulates the cell cycle and induces apoptosis, while inhibiting proliferation, migration, and invasion. These results highlight the

**Table 5 Relationships between clinicopathological factors of gastric cancer patients and anoctamin 5 expression**

Variables	N	IHC score		P value
		High group (1.3)	Low group (< 1.3)	
Total	195	58	137	
Sex	Male	35	93	0.3262
	Female	23	44	
Age	< 65	25	52	0.5246
	65	33	85	
Tumor location	U	15	26	0.3367
	M, L	43	111	
Tumor length (mm)	< 30	22	41	0.3158
	30	36	96	
Histological type	tub1, tub2, pap	35	61	0.0596
	por, sig, muc	23	76	
Lymphatic invasion	Negative	34	76	0.7529
	Positive	24	61	
Venous invasion	Negative	38	93	0.7419
	Positive	20	44	
pT	pT1-2	37	100	0.2312
	pT3-4	21	37	
pN	pN0	40	99	0.7294
	pN1-3	18	38	

IHC: Immunohistochemical; L: Lower; M: Middle; pap: muc: Mucinous adenocarcinoma; Papillary adenocarcinoma; pN: pathological N stage; por: Poorly differentiated adenocarcinoma; pT: pathological T stage; sig: Signet-ring cell carcinoma;tub: Tubular adenocarcinoma; U: Upper.

potential of ANO5 inhibitors as therapeutic agents for the treatment of GC or other cancer types with high ANO5 expression levels. The present study also indicates that ANO5 plays a key role in the proliferation of GC cells. Cell cycle analysis showed that the number of cells remaining in the G<sub>0</sub>/G<sub>1</sub> phase was significantly increased, whereas the number of cells in the S or G<sub>2</sub>/M phase was decreased in ANO5-depleted NUGC4 and MKN45 cells, suggesting that ANO5 downregulation inhibits GC cell proliferation *via* cell cycle arrest at the G<sub>0</sub>/G<sub>1</sub> phase.

The induction of p21 is dependent on the tumor suppressor protein, p53. However, chloride ions have been shown to play important roles in cell cycle progression by regulating the expression of p21 through a p53-independent pathway in GC cells[19]. It has also been demonstrated that a decrease in chloride induced G<sub>0</sub>/G<sub>1</sub> phase arrest by downregulating CDK2 and phosphorylated Rb expression through p21 upregulation. Furthermore, p38 and JNK activation under low-chloride conditions inhibits GC cell viability by upregulating p21 expression[18].

Moreover, ANO5 expression in GC cells affects the transition from the G<sub>1</sub> to the S phase of the cell cycle by regulating the expression of p21 and its downstream genes through the activation of JNK signaling. To the best of our knowledge, the chloride channel activity of ANO5 has not been confirmed to date. To elucidate the molecular mechanisms underlying the effects of ANO5, we evaluated the changes in the intracellular chloride ion environment in this study. A quantitative analysis of intracellular chloride ion concentrations was conducted based on the fluorescence intensity of MQAE. Immunofluorescent analysis showed that the fluorescence intensity of MQAE increased following ANO5 silencing, indicating a decrease in intracellular chloride concentration. These results suggest that the downregulation of ANO5 induces G<sub>0</sub>/G<sub>1</sub> phase arrest by altering the expression of G<sub>1</sub>/S checkpoint-related genes through the intracellular chloride environment of GC cells. Furthermore, since ANO5 functioned as a chloride channel, it may have the potential to inhibit tumor growth by regulating intracellular chloride concentrations in therapeutic settings.

Although ANO5 was recently implicated in various cancers, its role in tumor progression in patients with GC remains unclear. To demonstrate the clinical significance of ANO5 expression, the survival rate of 195 patients who underwent curative resection for primary GC was investigated. IHC analysis

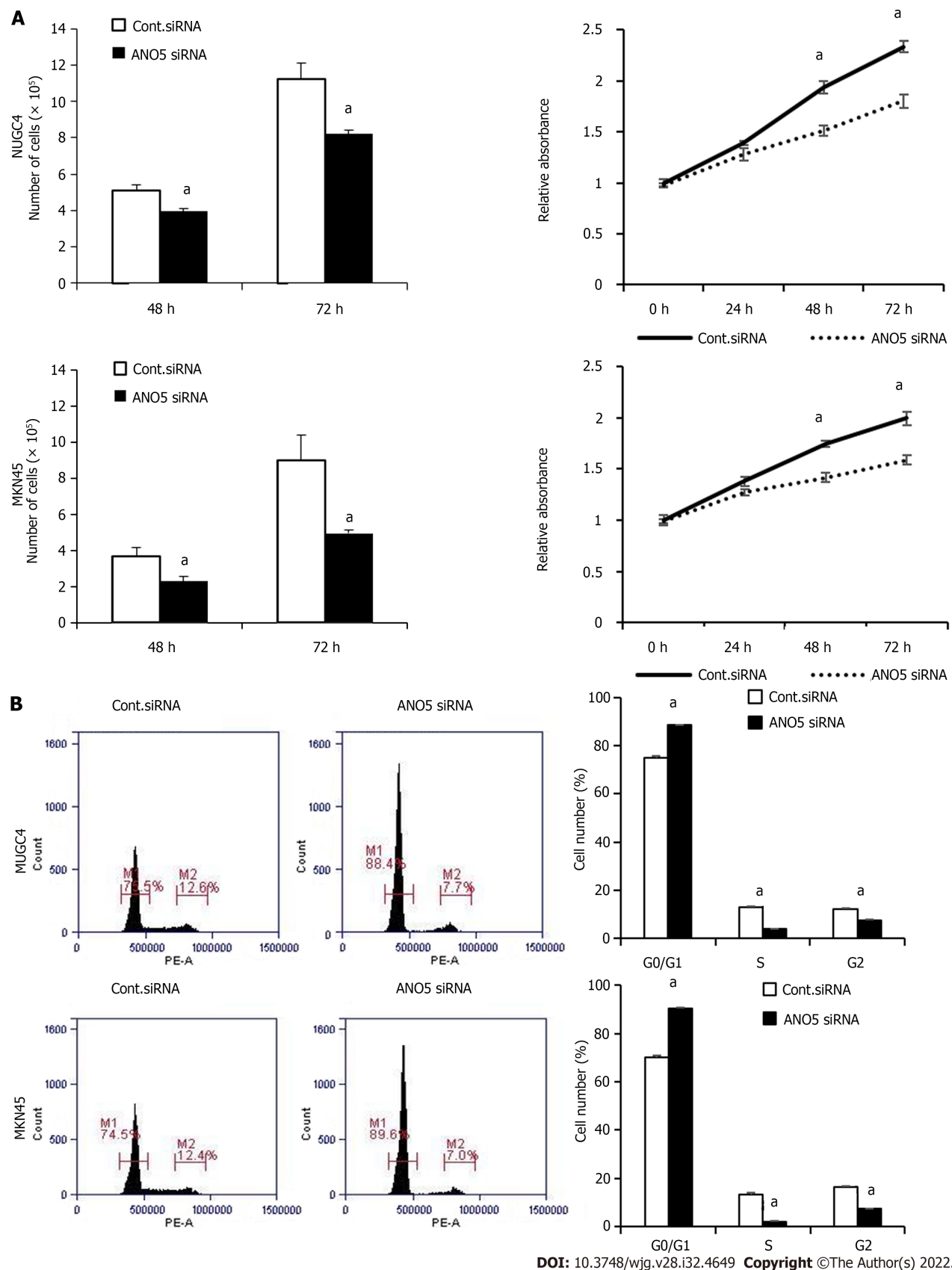
**Table 6 Univariate and multivariate analyses of prognostic factors associated with 5-year overall survival**

Variables	N	Univariate		Multivariate	
		5-yr OS rate (%)	P value	HR (95%CI)	P value
Total	195				
Sex					
Male	128	87.9	0.3274		
Female	67	85.3			
Age					
< 65	77	89.7	0.4113		
65	118	85.2			
Location					
U	41	80.9	0.2629		
M, L	154	88.6			
Tumor length (mm)					
< 30	63	97.8	0.0020 <sup>a</sup>	3.010 (0.347-26.12)	0.3176
30	132	80.1			
Histological type					
tub1, tub2, pap	96	88.3	0.4544		
por, sig, muc	99	85.6			
Lymphatic invasion					
Negative	110	96.1	0.0002 <sup>a</sup>	1.872 (0.549-6.384)	0.3166
Positive	85	75.7			
Venous invasion					
Negative	131	90.6	0.0126 <sup>a</sup>	1.085 (0.476-2.472)	0.8469
Positive	64	79.3			
pT					
pT1-2	137	95.9	< 0.0001 <sup>a</sup>	5.240 (1.807-15.20)	0.0023 <sup>c</sup>
pT3-4	58	65.5			
pN					
pN0	139	94.1	< 0.0001 <sup>a</sup>	2.148 (0.695-6.643)	0.1844
pN1-3	56	67.6			
IHC score					
< 1.3	137	89.6	0.0104 <sup>a</sup>	2.318 (1.016-5.288)	0.0457 <sup>c</sup>
1.3	58	73.9			

<sup>a</sup>P < 0.05: Log-rank test.<sup>c</sup>P < 0.05: Cox hazard regression analysis.

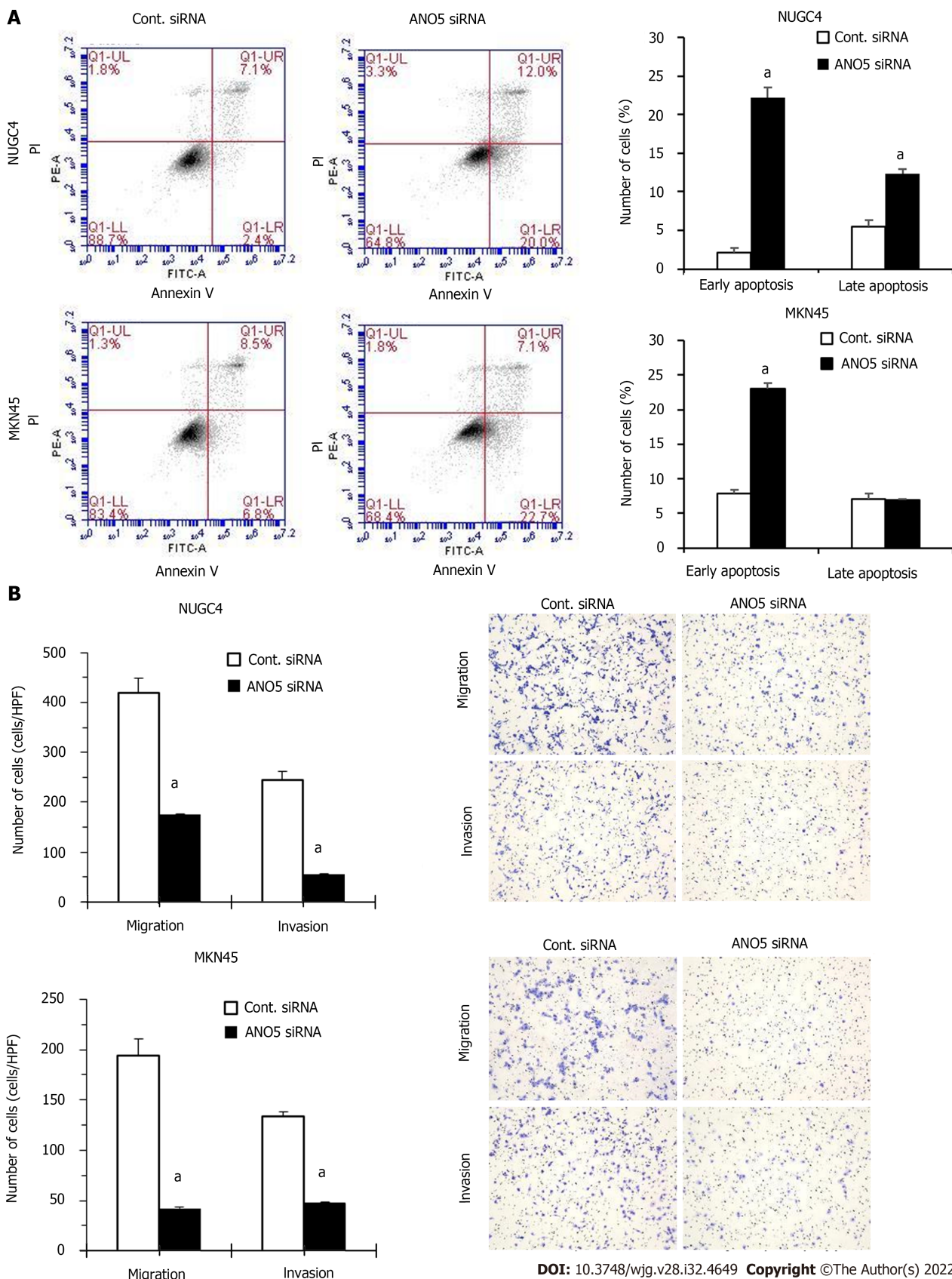
CI: Confidence interval; HR: Hazard ratio; IHC: Immunohistochemical; L: Lower; M: Middle; muc: Mucinous adenocarcinoma; OS: Overall survival; pap: Papillary adenocarcinoma; pN: Pathological N stage; por: Poorly differentiated adenocarcinoma; pT: Pathological T stage; sig: Signet-ring cell carcinoma; tub: Tubular adenocarcinoma; U: Upper.

revealed that high ANO5 expression levels were a poor prognostic factor in patients with GC. Under low-chloride conditions, ANO5 appeared to function as a chloride channel in GC cells. Previous findings showed that various ion transporters function as biomarkers and therapeutic targets[34,35]. Targeting ion channels that are activated in cancer cells may be an important strategy for cancer therapy. To the best of our knowledge, the present study is the first to report a relationship between ANO5 expression and the prognosis of patients with GC. Additional functional studies are needed to provide insights into the role of ANO5 in GC progression.

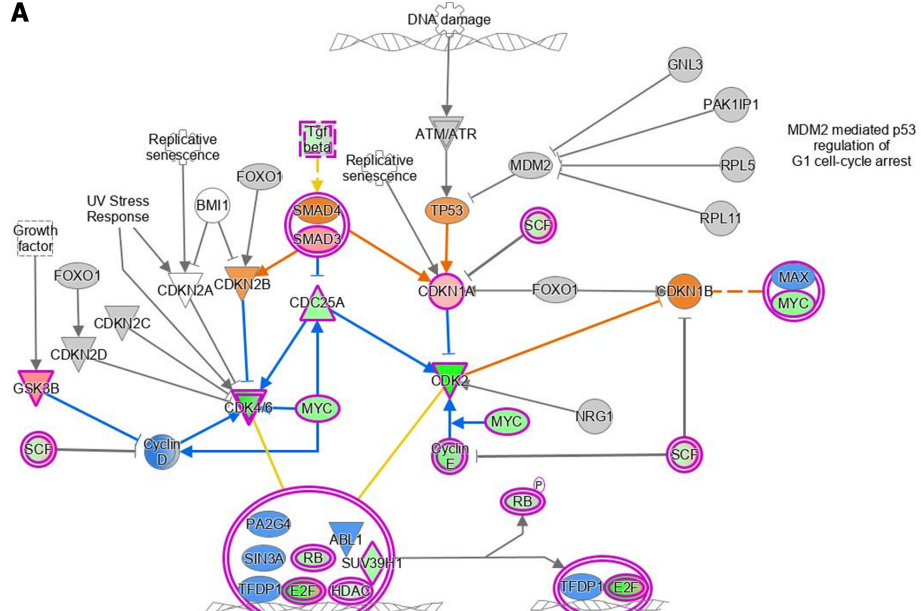
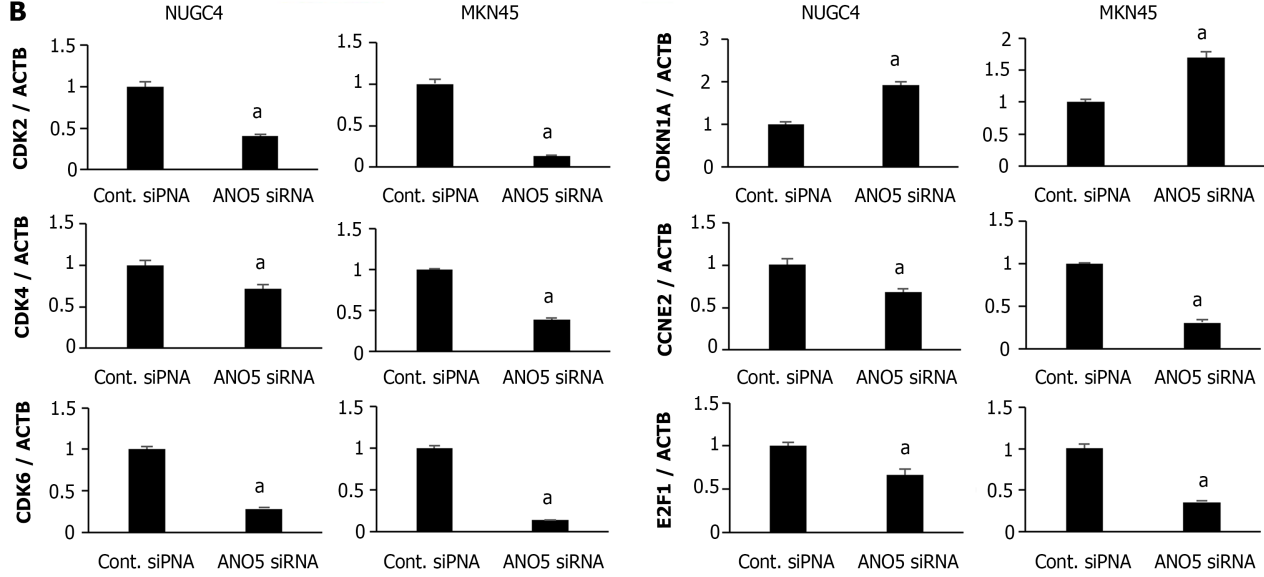
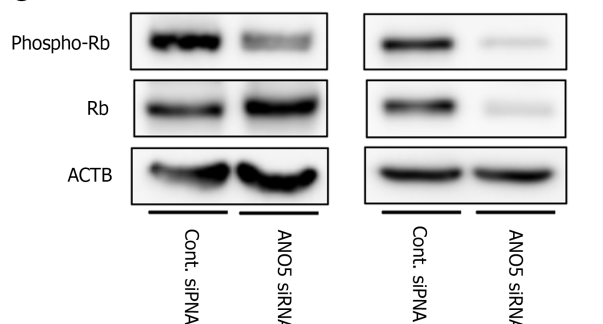
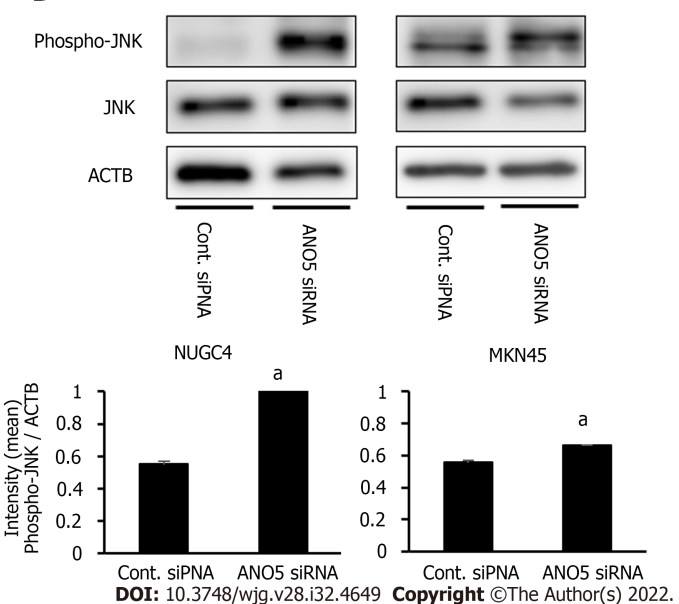


DOI: 10.3748/wjg.v28.i32.4649 Copyright ©The Author(s) 2022.

**Figure 2 Anoctamin 5 controlled the proliferation and the cell cycle in gastric cancer cells.** A: The downregulation of anoctamin 5 (ANO5) inhibited the proliferation of NUGC4 and MKN45 cells. Cell numbers were counted 48 h and 72 h after small interfering RNA transfection (left panel). The proliferative ability of NUGC4 and MKN45 cells was significantly suppressed following ANO5 downregulation (right panel); B: The downregulation of ANO5 increased the number of cells in the G<sub>0</sub>/G<sub>1</sub> phase in NUGC4 and MKN45 cells. Cells transfected with control or ANO5 small interfering RNA were stained with propidium iodide and analyzed by flow cytometry.  $n = 3$ , mean  $\pm$  standard error of the mean. <sup>a</sup> $P < 0.05$  (significantly different from control small interfering RNA). ANO5: Anoctamin 5; siRNA: Small interfering RNA; Cont.: Control.

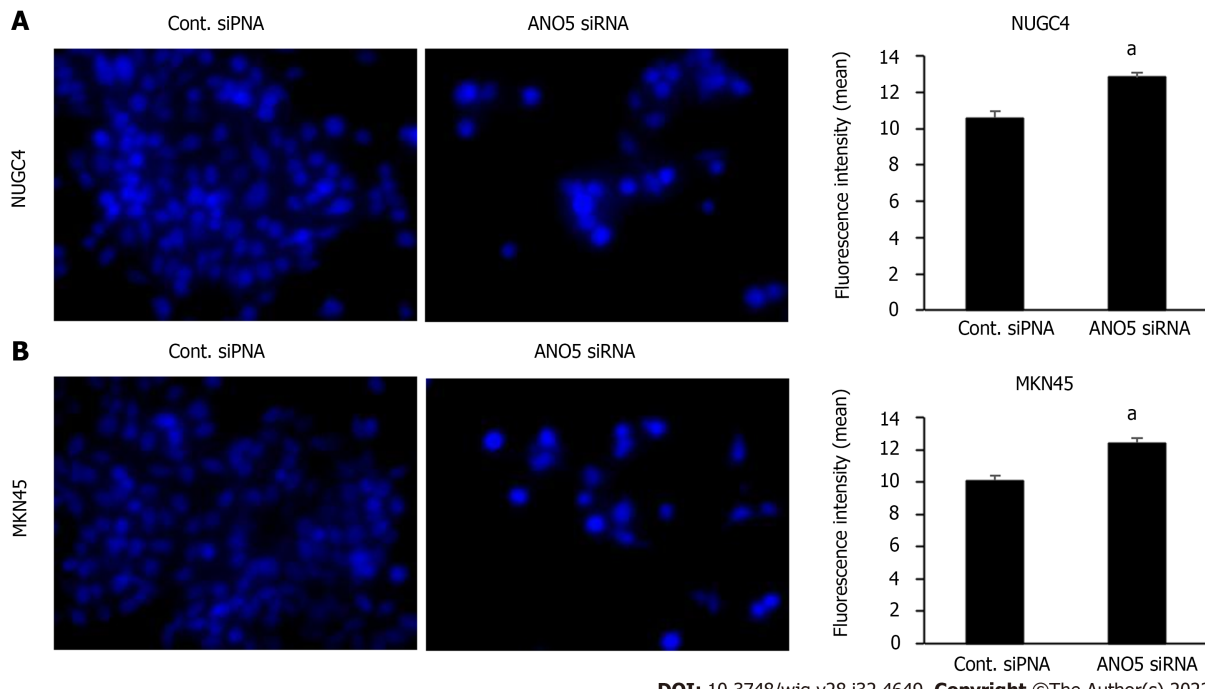


**Figure 3 Anoctamin 5 controlled apoptosis, migration, and invasion in gastric cancer cells.** A: The downregulation of anoctamin 5 (ANO5) increased the early and late apoptotic cell proportions of NUGC4 and MKN45 cells. Control or ANO5 small interfering RNA-transfected cells were stained with propidium iodide and annexin V and subjected to flow cytometry; B: The downregulation of ANO5 significantly decreased NUGC4 and MKN45 cell migration and invasion, which were evaluated using a Boyden chamber assay. Magnification:  $\times 40$ .  $n = 3$ , mean  $\pm$  standard error of the mean.  $^aP < 0.05$  (significantly different from control small interfering RNA). ANO5: Anoctamin 5; PI: Propidium iodide; siRNA: Small interfering RNA; Cont.: Control.

**A****B****C****D**

**Figure 4 Network analyses by microarray analysis and ingenuity pathway analysis.** A: The signaling map of "Cell Cycle: G<sub>1</sub>/S Checkpoint

Regulation," one of the top-ranked canonical pathways related to the depletion of anoctamin 5 (ANO5) according to ingenuity pathway analysis. Red and green colors indicate genes with expression levels that were higher or lower, respectively, than reference RNA levels; B: To verify gene expression profiling data, CDK2, CDK4, CDK6, CDKN1A, CCNE2, and E2F1 were examined by real-time reverse transcription-quantitative polymerase chain reaction. The downregulation of ANO5 effectively reduced CDK2, CDK4, CDK6, CCNE2, and E2F1 mRNA levels and increased CDKN1A/p21 mRNA levels in NUGC4 and MKN45 cells; C: The downregulation of ANO5 effectively reduced the phosphorylation levels of Rb protein in NUGC4 and MKN45 cells; D: The downregulation of ANO5 increased the phosphorylation of the c-Jun N-terminal kinase protein in NUGC4 and MKN45 cells.  $n = 3$ , mean  $\pm$  standard error of the mean.  $^aP < 0.05$  (significantly different from control small interfering RNA). ANO5: Anoctamin 5; siRNA: Small interfering RNA; Cont.: Control; JNK: c-Jun N-terminal kinase; ACTB:  $\beta$ -actin.



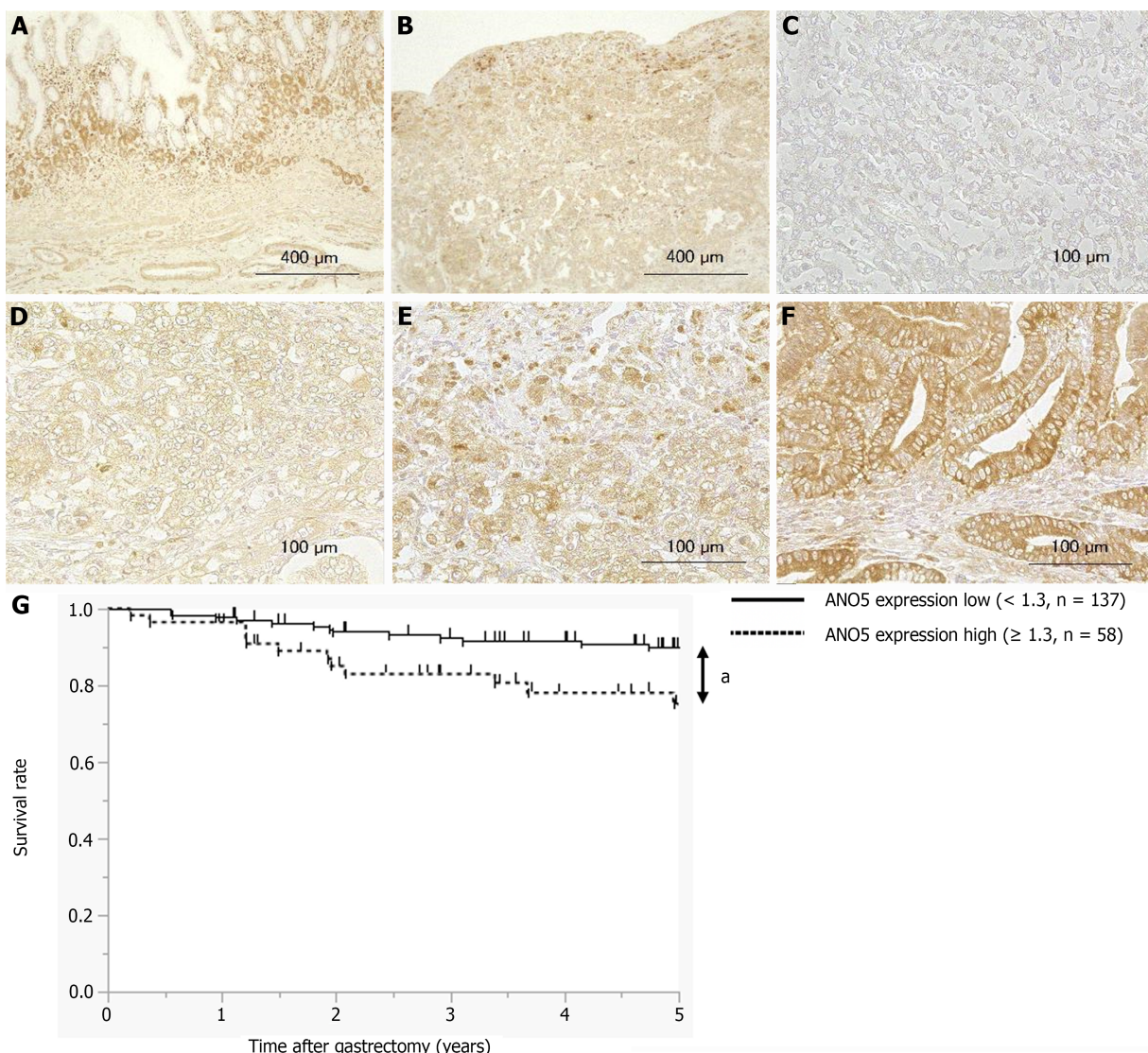
DOI: 10.3748/wjg.v28.i32.4649 Copyright ©The Author(s) 2022.

**Figure 5 Immunofluorescent analysis of intracellular chloride concentration using MQAE reagent, a chloride-sensitive fluorescence probe.** The downregulation of anoctamin 5 increased the fluorescence intensity of MQAE in NUGC4 and MKN45 cells. A: NUGC4 cell; B: MKN45 cell.  $n = 3$ , mean  $\pm$  standard error of the mean.  $^aP < 0.05$  (significantly different from control small interfering RNA). ANO5: Anoctamin 5; siRNA: Small interfering RNA; Cont.: Control.

This study has some limitations that must be addressed. First, it was a retrospective study. Due to the limited sample size, the pathological N stage classification factors were not correlated with the 5-year OS rate. Therefore, further studies are required to confirm our results. Second, in the selection of GC cell lines, we selected five cell lines; however, only three were used in the study.

## CONCLUSION

The present study revealed that ANO5 plays a significant role in cell cycle progression in human GC cells. The results of microarray analysis showed the impact of ANO5 on the expression of G<sub>1</sub>/S checkpoint-related genes. Furthermore, ANO5 expression significantly affected JNK signaling. Collectively, these results indicate that ANO5 plays an important role in cell cycle progression by regulating the expression of p21 through JNK signaling in human GC cells. The results of the IHC analysis also suggest that high ANO5 expression levels are a poor prognostic factor in patients with GC. The present study may contribute to the identification of ANO5 as a key mediator of tumor progression, with it ultimately being a promising prognostic biomarker or a novel therapeutic target for GC.



DOI: 10.3748/wjg.v28.i32.4649 Copyright ©The Author(s) 2022.

**Figure 6 Anoctamin 5 protein expression levels in human gastric cancer tissues and a survival analysis based on anoctamin 5 expression.** A: Non-cancerous gastric epithelia were immunohistochemically stained using an anti-anoctamin 5 (ANO5) antibody. Magnification:  $\times 100$ ; B: Primary human gastric cancer samples were immunohistochemically stained using an anti-ANO5 antibody. Magnification:  $\times 100$ ; C: The immunohistochemical staining results of ANO5 are shown as intensity 0. Magnification:  $\times 400$ ; D: Intensity 1. Magnification:  $\times 400$ ; E: Intensity 2. Magnification:  $\times 400$ ; F: Intensity 3. Magnification:  $\times 400$ ; G: Gastric cancer patients were classified into two groups based on ANO5 expression: A low ANO5 expression group ( $< 1.3$ ,  $n = 137$ ) and high ANO5 expression group ( $\geq 1.3$ ,  $n = 58$ ).  $^aP < 0.05$  (significant difference). ANO5: Anoctamin 5.

## ARTICLE HIGHLIGHTS

### Research background

Anoctamin 5 (ANO5) is a member of a family of calcium-activated chloride channels containing 10 members, also known as transmembrane proteins, and has been reported to be associated with various cancers.

### Research motivation

The role of ANO5 in gastric cancer (GC) remains poorly understood. In the present study, we analyzed the relationship between ANO5 expression and tumor progression in GC.

### Research objectives

The objectives of the present study were to investigate whether ANO5 contributes to the regulation of cancer growth and to clarify its clinicopathological significance in GC.

### Research methods

Knockdown experiments were performed by transfecting human GC cell lines with ANO5 small

interfering RNA. Gene expression was then assessed using microarray analysis. Samples from 195 patients with GC were subjected to immunohistochemistry for ANO5, and its relationship with clinicopathological factors and prognosis were examined.

### **Research results**

ANO5 knockdown suppressed the proliferation, migration, and invasion of cells and enhanced apoptosis. Cell cycle analysis showed that ANO5 knockdown suppressed the progression of G1-S phase. The results of microarray analysis showed up- or downregulated expression of genes related to "Cell Cycle: G1/S Checkpoint Regulation" in ANO5 knockdown NUGC4 cells. Survival analysis showed significantly poorer 5-year survival in the ANO5 high expression group (high vs low; 73.9 vs 89.6%,  $P = 0.0104$ ). Immunohistochemistry multivariate analysis identified the high expression of ANO5 as an independent prognostic factor for 5-year survival in GC patients ( $P = 0.0457$ ).

### **Research conclusions**

ANO5 plays a significant role in cell cycle progression in human GC cells. The results of the immunohistochemistry analysis suggest that high ANO5 expression levels are a poor prognostic factor in patients with GC.

### **Research perspectives**

The present study may contribute to the identification of ANO5 as a key mediator in tumor progression, with it ultimately being a promising prognostic biomarker or a novel therapeutic target of GC.

## **FOOTNOTES**

**Author contributions:** Fukami T and Shiozaki A contributed equally to this work; All authors read and approved the final manuscript and agreed to be accountable for all aspects of the report.

**Supported by** Japan Society for the Promotion of Science, No. 21K08689, No. 21K16456, No. 20K09016, No. 20K09084, No. 19K09202 and No. 19K09182.

**Institutional review board statement:** The study was reviewed and approved by the Kyoto Prefectural University of Medicine Institutional Review Board, No. ERB-C-1195.

**Informed consent statement:** Informed consent to be included in the study, or the equivalent, was obtained from all patients.

**Conflict-of-interest statement:** All the authors report no relevant conflicts of interest for this article.

**Data sharing statement:** Technical appendix, statistical code, and dataset available from the corresponding author at [shiozaki@koto.kpu-m.ac.jp](mailto:shiozaki@koto.kpu-m.ac.jp). Participants gave informed consent for data sharing.

**Open-Access:** This article is an open-access article that was selected by an in-house editor and fully peer-reviewed by external reviewers. It is distributed in accordance with the Creative Commons Attribution NonCommercial (CC BY-NC 4.0) license, which permits others to distribute, remix, adapt, build upon this work non-commercially, and license their derivative works on different terms, provided the original work is properly cited and the use is non-commercial. See: <https://creativecommons.org/Licenses/by-nc/4.0/>

**Country/Territory of origin:** Japan

**ORCID number:** Tomoyuki Fukami [0000-0002-2585-3611](#); Atsushi Shiozaki [0000-0003-3739-160X](#); Toshiyuki Kosuga [0000-0002-1657-7272](#); Michihiro Kudou [0000-0003-3518-528X](#); Hiroki Shimizu [0000-0002-6463-8498](#); Takuma Ohashi [0000-0003-0939-3739](#); Tomohiro Arita [0000-0001-7127-6504](#); Hirotaka Konishi [0000-0002-4899-8944](#); Shuhei Komatsu [0000-0001-6074-7614](#); Takeshi Kubota [0000-0002-2246-3028](#); Hitoshi Fujiwara [0000-0002-6507-4313](#); Kazuma Okamoto [0000-0002-8270-4217](#); Mitsuo Kishimoto [0000-0002-7407-9044](#); Yukiko Morinaga [0000-0003-2311-1830](#); Eiichi Konishi [0000-0002-7122-2271](#); Eigo Otsuji [0000-0002-3260-8155](#).

**S-Editor:** Fan JR

**L-Editor:** Filopodia

**P-Editor:** Cai YX

## **REFERENCES**

- 1 Pang C, Yuan H, Ren S, Chen Y, An H, Zhan Y. TMEM16A/B associated CaCC: structural and functional insights.

- Protein Pept Lett* 2014; **21**: 94-99 [PMID: 24151904 DOI: 10.2174/09298665113206660098]
- 2 **Pedemonte N**, Galietta LJ. Structure and function of TMEM16 proteins (anoctamins). *Physiol Rev* 2014; **94**: 419-459 [PMID: 24692353 DOI: 10.1152/physrev.00039.2011]
  - 3 **Whitlock JM**, Hartzell HC. Anoctamins/TMEM16 Proteins: Chloride Channels Flirting with Lipids and Extracellular Vesicles. *Annu Rev Physiol* 2017; **79**: 119-143 [PMID: 27860832 DOI: 10.1146/annurev-physiol-022516-034031]
  - 4 **Schreiber R**, Uliyakina I, Kongsuphol P, Warth R, Mirza M, Martins JR, Kunzelmann K. Expression and function of epithelial anoctamins. *J Biol Chem* 2010; **285**: 7838-7845 [PMID: 20056604 DOI: 10.1074/jbc.M109.065367]
  - 5 **Kunzelmann K**. TMEM16, LRRC8A, bestrophin: chloride channels controlled by Ca(2+) and cell volume. *Trends Biochem Sci* 2015; **40**: 535-543 [PMID: 26254230 DOI: 10.1016/j.tibs.2015.07.005]
  - 6 **Wanitchakool P**, Wolf L, Koehl GE, Sirianant L, Schreiber R, Kulkarni S, Duvvuri U, Kunzelmann K. Role of anoctamins in cancer and apoptosis. *Philos Trans R Soc Lond B Biol Sci* 2014; **369**: 20130096 [PMID: 24493744 DOI: 10.1098/rstb.2013.0096]
  - 7 **Miettinen M**. Immunohistochemistry of soft tissue tumours - review with emphasis on 10 markers. *Histopathology* 2014; **64**: 101-118 [PMID: 24111893 DOI: 10.1111/his.12298]
  - 8 **Lu G**, Shi W, Zheng H. Inhibition of STAT6/Anoctamin-1 Activation Suppresses Proliferation and Invasion of Gastric Cancer Cells. *Cancer Biother Radiopharm* 2018; **33**: 3-7 [PMID: 29466035 DOI: 10.1089/cbr.2017.2287]
  - 9 **Shang L**, Hao JJ, Zhao XK, He JZ, Shi ZZ, Liu HJ, Wu LF, Jiang YY, Shi F, Yang H, Zhang Y, Liu YZ, Zhang TT, Xu X, Cai Y, Jia XM, Li M, Zhan QM, Li EM, Wang LD, Wei WQ, Wang MR. ANO1 protein as a potential biomarker for esophageal cancer prognosis and precancerous lesion development prediction. *Oncotarget* 2016; **7**: 24374-24382 [PMID: 27016410 DOI: 10.18632/oncotarget.8223]
  - 10 **Jia L**, Liu W, Guan L, Lu M, Wang K. Inhibition of Calcium-Activated Chloride Channel ANO1/TMEM16A Suppresses Tumor Growth and Invasion in Human Lung Cancer. *PLoS One* 2015; **10**: e0136584 [PMID: 26305547 DOI: 10.1371/journal.pone.0136584]
  - 11 **Bill A**, Gutierrez A, Kulkarni S, Kemp C, Bonenfant D, Voshol H, Duvvuri U, Gaither LA. ANO1/TMEM16A interacts with EGFR and correlates with sensitivity to EGFR-targeting therapy in head and neck cancer. *Oncotarget* 2015; **6**: 9173-9188 [PMID: 25823819 DOI: 10.18632/oncotarget.3277]
  - 12 **Britschgi A**, Bill A, Brinkhaus H, Rothwell C, Clay I, Duss S, Rebhan M, Raman P, Guy CT, Wetzel K, George E, Popa MO, Lilley S, Choudhury H, Gosling M, Wang L, Fitzgerald S, Borawski J, Baffoe J, Labow M, Gaither LA, Bentires-Alj M. Calcium-activated chloride channel ANO1 promotes breast cancer progression by activating EGFR and CAMK signaling. *Proc Natl Acad Sci U S A* 2013; **110**: E1026-E1034 [PMID: 23431153 DOI: 10.1073/pnas.1217072110]
  - 13 **Duran C**, Hartzell HC. Physiological roles and diseases of Tmem16/Anoctamin proteins: are they all chloride channels? *Acta Pharmacol Sin* 2011; **32**: 685-692 [PMID: 21642943 DOI: 10.1038/aps.2011.48]
  - 14 **Dutertre M**, Lacroix-Triki M, Driouch K, de la Grange P, Gratadou L, Beck S, Millevoi S, Tazi J, Lidereau R, Vagner S, Auboeuf D. Exon-based clustering of murine breast tumor transcriptomes reveals alternative exons whose expression is associated with metastasis. *Cancer Res* 2010; **70**: 896-905 [PMID: 20103641 DOI: 10.1158/0008-5472.CAN-09-2703]
  - 15 **Li Y**, Wang X, Vural S, Mishra NK, Cowan KH, Guda C. Exome analysis reveals differentially mutated gene signatures of stage, grade and subtype in breast cancers. *PLoS One* 2015; **10**: e0119383 [PMID: 25803781 DOI: 10.1371/journal.pone.0119383]
  - 16 **Jun I**, Park HS, Piao H, Han JW, An MJ, Yun BG, Zhang X, Cha YH, Shin YK, Yook JI, Jung J, Gee HY, Park JS, Yoon DS, Jeung HC, Lee MG. ANO9/TMEM16J promotes tumourigenesis via EGFR and is a novel therapeutic target for pancreatic cancer. *Br J Cancer* 2017; **117**: 1798-1809 [PMID: 29024940 DOI: 10.1038/bjc.2017.355]
  - 17 **Li C**, Cai S, Wang X, Jiang Z. Identification and characterization of ANO9 in stage II and III colorectal carcinoma. *Oncotarget* 2015; **6**: 29324-29334 [PMID: 26317553 DOI: 10.18632/oncotarget.4979]
  - 18 **Shiozaki A**, Otsuji E, Marunaka Y. Intracellular chloride regulates the G(1)/S cell cycle progression in gastric cancer cells. *World J Gastrointest Oncol* 2011; **3**: 119-122 [PMID: 22007274 DOI: 10.4251/wjgo.v3.i8.119]
  - 19 **Miyazaki H**, Shiozaki A, Niisato N, Ohsawa R, Itoi H, Ueda Y, Otsuji E, Yamagishi H, Iwasaki Y, Nakano T, Nakahari T, Marunaka Y. Chloride ions control the G1/S cell-cycle checkpoint by regulating the expression of p21 through a p53-independent pathway in human gastric cancer cells. *Biochem Biophys Res Commun* 2008; **366**: 506-512 [PMID: 18067855 DOI: 10.1016/j.bbrc.2007.11.144]
  - 20 **Shiozaki A**, Miyazaki H, Niisato N, Nakahari T, Iwasaki Y, Itoi H, Ueda Y, Yamagishi H, Marunaka Y. Furosemide, a blocker of Na+/K+/2Cl- cotransporter, diminishes proliferation of poorly differentiated human gastric cancer cells by affecting G0/G1 state. *J Physiol Sci* 2006; **56**: 401-406 [PMID: 17052386 DOI: 10.2170/physiolsci.RP010806]
  - 21 **Kurashima K**, Shiozaki A, Kudou M, Shimizu H, Arita T, Kosuga T, Konishi H, Komatsu S, Kubota T, Fujiwara H, Okamoto K, Kishimoto M, Konishi E, Otsuji E. LRRC8A influences the growth of gastric cancer cells via the p53 signaling pathway. *Gastric Cancer* 2021; **24**: 1063-1075 [PMID: 33864161 DOI: 10.1007/s10120-021-01187-4]
  - 22 **Chang Z**, Cai C, Han D, Gao Y, Li Q, Feng L, Zhang W, Zheng J, Jin J, Zhang H, Wei Q. Anoctamin5 regulates cell migration and invasion in thyroid cancer. *Int J Oncol* 2017; **51**: 1311-1319 [PMID: 28902351 DOI: 10.3892/ijo.2017.4113]
  - 23 **Song HY**, Zhou L, Hou XF, Lian H. Anoctamin 5 regulates cell proliferation and migration in pancreatic cancer. *Int J Clin Exp Pathol* 2019; **12**: 4263-4270 [PMID: 31933826]
  - 24 **James DB**, Mary KG, Christian W. International Union Against Cancer (UICC) TNM classification of malignant tumors. 8th edition. Wiley: New York, 2017
  - 25 **Kim GY**, Mercer SE, Ewton DZ, Yan Z, Jin K, Friedman E. The stress-activated protein kinases p38 alpha and JNK1 stabilize p21(Cip1) by phosphorylation. *J Biol Chem* 2002; **277**: 29792-29802 [PMID: 12058028 DOI: 10.1074/jbc.M201299200]
  - 26 **Mazumdar M**, Glassman JR. Categorizing a prognostic variable: review of methods, code for easy implementation and applications to decision-making about cancer treatments. *Stat Med* 2000; **19**: 113-132 [PMID: 10623917 DOI: 10.1002/(sici)1097-0258(20000115)19:1<113::aid-sim245>3.0.co;2-0]
  - 27 **Suzuki J**, Umeda M, Sims PJ, Nagata S. Calcium-dependent phospholipid scrambling by TMEM16F. *Nature* 2010; **468**: 834-838 [PMID: 21107324 DOI: 10.1038/nature09583]

- 28 **Huang F**, Wang X, Ostertag EM, Nuwal T, Huang B, Jan YN, Basbaum AI, Jan LY. TMEM16C facilitates Na(+) -activated K<sup>+</sup> currents in rat sensory neurons and regulates pain processing. *Nat Neurosci* 2013; **16**: 1284-1290 [PMID: 23872594 DOI: 10.1038/nn.3468]
- 29 **Caputo A**, Caci E, Ferrera L, Pedemonte N, Barsanti C, Sondo E, Pfeffer U, Ravazzolo R, Zegarra-Moran O, Galietta LJ. TMEM16A, a membrane protein associated with calcium-dependent chloride channel activity. *Science* 2008; **322**: 590-594 [PMID: 18772398 DOI: 10.1126/science.1163518]
- 30 **Schroeder BC**, Cheng T, Jan YN, Jan LY. Expression cloning of TMEM16A as a calcium-activated chloride channel subunit. *Cell* 2008; **134**: 1019-1029 [PMID: 18805094 DOI: 10.1016/j.cell.2008.09.003]
- 31 **Yang YD**, Cho H, Koo JY, Tak MH, Cho Y, Shim WS, Park SP, Lee J, Lee B, Kim BM, Raouf R, Shin YK, Oh U. TMEM16A confers receptor-activated calcium-dependent chloride conductance. *Nature* 2008; **455**: 1210-1215 [PMID: 18724360 DOI: 10.1038/nature07313]
- 32 **Terashima H**, Picollo A, Accardi A. Purified TMEM16A is sufficient to form Ca2+-activated Cl<sup>-</sup> channels. *Proc Natl Acad Sci U S A* 2013; **110**: 19354-19359 [PMID: 24167264 DOI: 10.1073/pnas.1312014110]
- 33 **Song HY**, Tian YM, Zhang YM, Zhou L, Lian H, Zhu JX. A novel finding of anoctamin 5 expression in the rodent gastrointestinal tract. *Biochem Biophys Res Commun* 2014; **451**: 258-262 [PMID: 25094048 DOI: 10.1016/j.bbrc.2014.07.121]
- 34 **Siveen KS**, Nizamuddin PB, Uddin S, Al-Thani M, Frenneaux MP, Janahi IA, Steinhoff M, Azizi F. TRPV2: A Cancer Biomarker and Potential Therapeutic Target. *Dis Markers* 2020; **2020**: 8892312 [PMID: 33376561 DOI: 10.1155/2020/8892312]
- 35 **Xu R**, Wang X, Shi C. Volume-regulated anion channel as a novel cancer therapeutic target. *Int J Biol Macromol* 2020; **159**: 570-576 [PMID: 32442571 DOI: 10.1016/j.ijbiomac.2020.05.137]



Published by **Baishideng Publishing Group Inc**  
7041 Koll Center Parkway, Suite 160, Pleasanton, CA 94566, USA

**Telephone:** +1-925-3991568

**E-mail:** [bpgoffice@wjnet.com](mailto:bpgoffice@wjnet.com)

**Help Desk:** <https://www.f6publishing.com/helpdesk>

<https://www.wjnet.com>

